

Surface and Chemical Study of $\text{SiO}_2 \cdot \text{P}_2\text{O}_5 \cdot \text{CaO} \cdot (\text{MgO})$ Bioactive Glasses

J. Pérez-Pariente, F. Balas, and M. Vallet-Regí*

Departamento de Química Inorgánica y Bioinorgánica, Facultad de Farmacia, Universidad Complutense de Madrid, Plaza de Ramón y Cajal, 28040 Madrid, Spain

Received July 29, 1999. Revised Manuscript Received October 25, 1999

Glasses in $\text{SiO}_2 \cdot \text{CaO} \cdot \text{P}_2\text{O}_5$ and $\text{SiO}_2 \cdot \text{CaO} \cdot \text{P}_2\text{O}_5 \cdot \text{MgO}$ systems have been prepared by a sol–gel synthesis procedure. The calcined glasses have been characterized by XRD, N_2 adsorption, Hg porosimetry, XPS and TEM and have been also subjected to in vitro tests (immersion in a simulated body fluid) to evaluate their bioactivity. The presence of magnesium in the glasses increases the surface area and porosity, but it retards the formation of an apatite layer on the surface of glasses in the in vitro test. The XPS reveals that the surfaces of the glasses are richer in phosphorus and poorer in calcium than the bulk, whereas the magnesium, if present, associates preferentially to phosphorus at the glass surface. The TEM shows the presence of apatite-like calcium phosphate domains in the magnesium-free glasses, which are barely detected in the glasses, which contain this element. These apatitic domains are proposed to be the nucleation centers for the crystallization of apatite in the in vitro tests.

Introduction

The formation of a calcium phosphate layer on bioactive glasses when they are immersed in a simulated body fluid (SBF)^{1,2} is a complex phenomenon, which could depend on both chemical and textural parameters (surface area and porosity) of the substrate. In the particular case of glasses prepared by a sol–gel procedure, their high surface area has been claimed as responsible for the growing of an apatite layer on the surface.³ Furthermore, the presence of pores sizes >2 nm is required to achieve rapid crystallization of this apatite layer.⁴

Although the influence of the texture of the substrate on the formation of apatite is generally admitted, the detailed nature of the nucleation process of the apatite is still a matter of debate. The practical totality of authors focuses the discussion on apatite nucleation upon the role of the silanol groups existing on the glass surface under the environmental conditions where the essays are conducted.^{4–7} More recently, Wang and Chaki⁸ show an epitaxial relationship between Si(111) and apatite in [102] orientation. Interestingly, the

phosphorus and calcium of the substrate are generally considered as a mere reservoir that influences the supersaturation of the solution as they are leached from the glass. It is remarkable that neither phosphorus nor calcium pertaining to the glass is ever considered as potential nucleation centers for apatite crystallization. Indeed, the information regarding the chemical state of phosphorus in bioactive glasses is very scarce, despite of the importance that this element may have when considering the formation of a calcium phosphate layer onto the surface.

To gain knowledge on the influence that the chemical nature of the glass surface has on the nucleation events leading to the formation of apatite, here we report the results we have obtained in the study of the relationship between the in vitro bioactivity of $\text{SiO}_2 \cdot \text{CaO} \cdot \text{P}_2\text{O}_5 \cdot (\text{MgO})$ sol–gel glasses and the textural properties and chemical nature of the glass surface.

Experimental Section

Preparation of the Glasses. Four different glasses, two with different SiO_2 contents, 65 and 75 mol %, one with CaO, and one with CaO and MgO ($\text{Ca/Mg} = 4.1$) (4 mol % of P_2O_5 in all cases) were prepared by hydrolysis and polycondensation of tetraethyl orthosilicate (TEOS), triethyl phosphate (TEP), calcium nitrate, and, in two samples, also magnesium nitrate, in the presence of water (mole of $\text{H}_2\text{O}/(\text{mole of TEOS} + \text{mole of TEP}) = 8$). Nitric acid was added to catalyze the hydrolysis and condensation of alkoxides (mole of $\text{HNO}_3/(\text{mole of TEOS} + \text{mole of TEP}) = 0.05$). The synthesis procedure, the same for all the compositions, was as follows: the TEOS is mixed with water and 2 N HNO_3 , and then the TEP, calcium nitrate, and magnesium nitrate, if required, were successively added, by keeping 1 h intervals between additions. In every case, after the reactants were mixed, the sol was introduced into polyethylene containers where it was allowed to gel at room temperature and then aged at 70 °C for 3 days and dried at 150 °C for 2 days. The resulting glasses are denoted as 65S, 75S (magnesium free samples), 65SM, and 75SM (samples

(1) Kokubo, T.; Kushitani, H.; Sakka, S.; Kitsugi, T.; Yamamuro, T. *J. Biomed. Mater. Res.* **1990**, *24*, 721.

(2) Ohtsuki, C.; Kokubo, T.; Yamamuro, T. *J. Non-Cryst. Solids* **1992**, *143*, 84.

(3) Li, R.; Clark, A. E.; Hench, L. L. *J. Appl. Biomater.* **1991**, *2*, 231.

(4) Pereira, M. M.; Hench, L. L. *J. Sol-Gel Sci. Technol.* **1996**, *7*, 59.

(5) Li, P.; Ohtsuki, C.; Kokubo, T.; Nakanishi, K.; Soga, N.; Nakamura, T.; Yamamuro, T. *J. Am. Ceram. Soc.* **1992**, *75*, 2094.

(6) Karlsson, K. H.; Froberg, K.; Ringbom, T. *J. Non-Cryst. Solids* **1989**, *112*, 69.

(7) Kokubo, T.; Cho, S. B.; Nakanishi, K.; Soga, N.; Ohtsuki, C.; Kitsugi, T.; Yamamuro, T.; Nakamura, T. In *Bioceramics*; Andersson, Ö. H., Yli-Urpo, A., Eds.; Butterworth-Heinemann Ltd: Oxford, 1994; Vol. 7, p 49.

(8) Wang, P. E.; Chaki, T. K. *J. Mater. Sci. Mater. Med.* **1995**, *6*, 94.

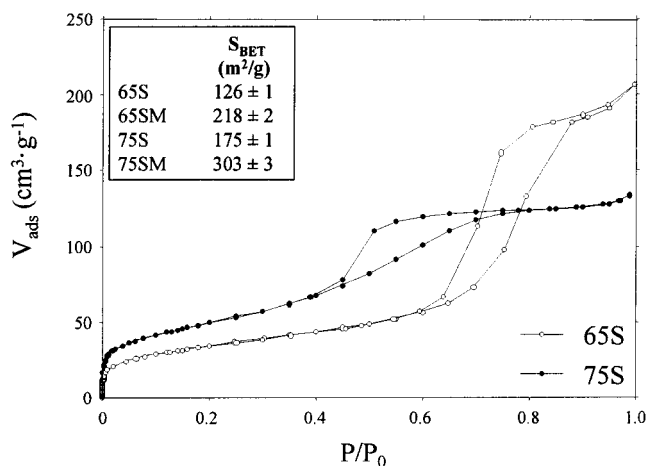


Figure 1. N₂ adsorption isotherms of SiO₂-P₂O₅-CaO glasses. Surface areas of the four glasses are given in the inset.

with magnesium), where the number corresponds to the SiO₂ content in mole %.

In Vitro Bioactivity Test. The calcined glasses were subjected to in vitro tests to evaluate their bioactivity. Fractions of 500 mg of glass powders were pressed in air using a uniaxial press and a steel die with an applied pressure of 55 MPa, and then isostatically pressed at 150 MPa for 3 min and calcined at 600 °C for 3 h. The so-obtained disks (13 mm diameter, 2 mm thickness) were mounted vertically in a special Pt scaffold, and soaked in 45 mL of simulated body fluid solution (SBF) in polyethylene containers maintained at 37 °C. The chemical composition of the SBF solution is that described in ref 9.

Formation of apatite-like layer on sintered disks was determined by X-ray diffraction (XRD) by using a Philips X'Pert MPD diffractometer and Cu K α radiation. N₂ adsorption was carried out on a Micromeritics ASAP 2000 instrument. Surface area was obtained by applying the BET method to the isotherm. Pore size distribution was determined by the BJH method from the desorption branch of the isotherm. Hg porosimetry was done on a Micromeritics Autopore III 9420 instrument. Pore sizes in the range from 100 μ m to 3 nm were determined by this technique.

For TEM observations and ED studies, samples scraped from the surface of glass disks were dispersed in 1-butanol and then transferred to carbon-coated copper grids. The examinations were performed on a JEOL 2000 FX electron microscope working at 200 kV.

Chemical analysis of the surface was determined by X-ray photoelectron spectroscopy (XPS) with an Escalab-210 spectrometer. Binding energies were corrected for charge effects by referring to the carbon 1s peak at 284.9 eV. This measurement was carried out on the calcined monolithic disks.

Results and Discussion

Textural Properties. Having taken into account that all the four sol-gel glasses were synthesized using the same preparation parameters, the porosity and textural properties of samples will be discussed as a function of composition.

The N₂ adsorption isotherms of the glasses that do not contain magnesium are plotted in Figure 1. These isotherms are similar to those of magnesium-containing glasses. They correspond to the type IV isotherm according to the BDDT classification.¹⁰ The characteristic

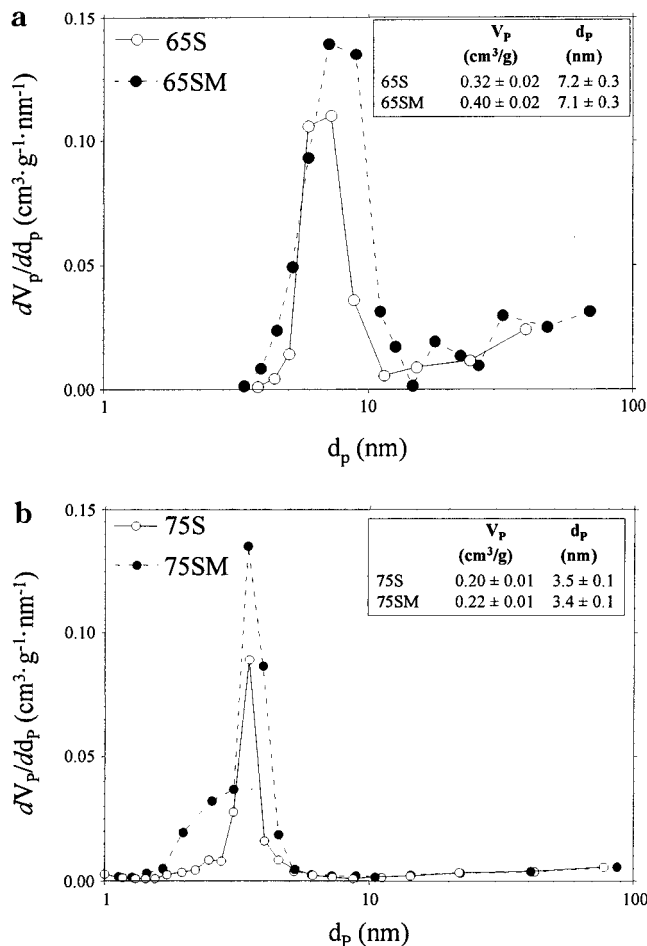


Figure 2. Pore size distribution and porosity of glasses by N₂ adsorption (BJH method).

hysteresis loop of this isotherm can be observed in all cases, i.e., desorption branch does not follow the same path as the adsorption branch at relatively high P/P_0 values. This behavior clearly indicates the presence of mesopores in the solids. The hysteresis loop shifts toward lower P/P_0 values as the silica content of the glasses increase, which can be taken as an evidence of a reduction of the average pore size. Furthermore, it can also be observed that the magnesium has little influence in the shape of the isotherm for given silica content. This is reflected in the pore size distribution obtained from the desorption branch of the isotherm following the BJH method (Figure 2). The four glasses show a monomodal and narrow pore size distribution in the mesopore range ($2 < d_p < 50$ nm). The average pore size decreases from 7 to 3 nm as the silica content increases from 65 to 75%, but it is little affected by the presence of magnesium (see insets in Figure 2). On the other hand, the t plot analysis of the isotherm indicates the absence of micropores ($d_p < 2$ nm) in all cases.

The BET surface area increases with the silica content of the glass, and it is also enhanced by the presence of magnesium. The glasses also have a high pore volume, which nevertheless decreases, as the samples become richer in silica.

The pore size distributions in the meso- and macropore region determined from Hg porosimetry are given in Figure 3. The samples exhibit a bimodal pattern of porosity, with two maxima centered in the mesopore

(9) Cho, S. B.; Nakanishi, K.; Kokubo, T.; Soga, N.; Ohtsuki, C.; Nakamura, T.; Kitsugi, T.; Yamamuro, T. *J. Am. Ceram. Soc.* **1995**, *78*, 1769.

(10) Gregg, S. J.; Sing, K. S. W. *Adsorption, Surface Area and Porosity*; Academic Press: New York, 1982; p 1.

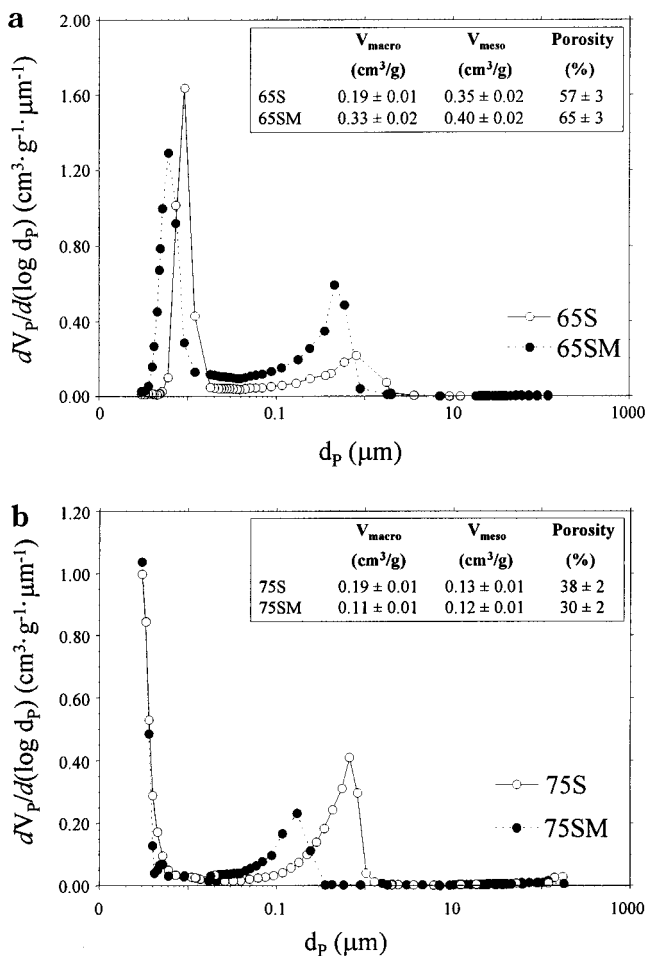


Figure 3. Pore size distribution and porosity of glasses in the mesopore and macropore ranges determined by Hg porosimetry.

region, below 10 nm, and in the macropore region, in the range from 10^4 to 10^2 nm. The sharp maxima in the mesopore range correspond closely with the pores detected by N_2 adsorption (Figure 2). For the samples with 75% silica, only the ascendant branch of the pore size distribution is observed. This behavior is due to the presence of pores so small that mercury cannot penetrate all of them, since the detection limit of this technique is 3 nm. As a consequence, the total porosity of the glasses richest in silica is underestimated by Hg porosimetry.

It can be observed in Figure 3 that the overall pore distribution shifts toward lower sizes as the silica increases. Also, for each silica content, the addition of magnesium to the glass also reduces the average pore size of the macropores, this effect being more pronounced for the sample with 75% of silica. On the other hand, practically no pores below $\sim 2 \mu\text{m}$ in size are detected in the four glasses.

To summarize the results referring the texture of the glasses, it can be said that the porosity in the mesopore region is influenced by the silica content of the material, whereas the magnesium content enhances the surface area and also affects the macroporosity. Therefore, the addition of magnesium to the glass does not seem to have a deleterious influence on properties that are relevant for bioactivity, namely surface area and porosity.

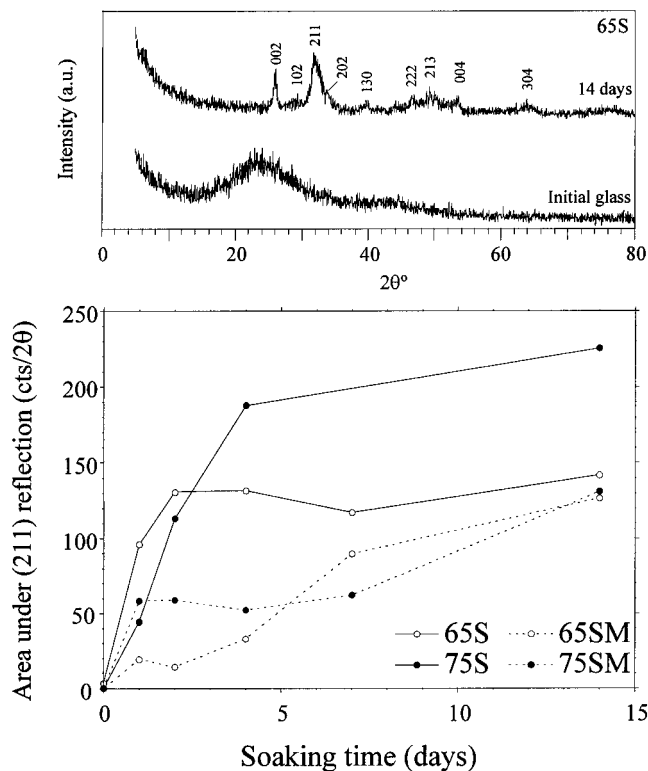


Figure 4. Area under (211) reflection of the apatite phase vs soaking time (bottom). XRD patterns of the 65S glass before and after 14 weeks of soaking (top).

In Vitro Test. When the disks of glass are soaked into the SBF solution, the formation of an apatite-like layer is detected by XRD. Plotting the area of the (211) reflection as a function of the immersion time can conveniently monitor the growth rate of this layer. The results obtained for the four glasses are presented in the Figure 4. Strong differences in growth rate between the different samples are observed in the figure. The highest rate of apatite formation takes place on the glasses that do not contain magnesium (65S and 75S). A faster crystallization rate is found for the glass richer in calcium (65S), but the formation of the phosphate layer is more quantitative for the sample 75S. Partial replacement of calcium by magnesium provokes a strong reduction in the initial crystal growth rate, but nevertheless a continuous increase of the apatite layer with time is observed in both cases.

A detailed analysis of the rate of apatite formation should take into account factors dependent on the surface of the glass but also the chemical composition of the liquid phase. The calcium concentration in the solution as a function of the soaking time is given in Figure 5. The leaching of this ion to the solution is higher for the glasses richest in this element (65S and 65SM), but its concentration stabilizes after ~ 7 days. The higher leaching rate of Ca^{2+} from the 65S substrate at short soaking times as compared with 75S might account for the faster crystallization of apatite on this glass (Figure 4), but it can hardly explain the continuous progress of the apatite layer on the 75S beyond 2 days. Other factors, such as the higher surface area of the glass 75S, might account for this behavior.

The influence of the magnesium present in the glass, on the concentration of Ca^{2+} in the solution, is very

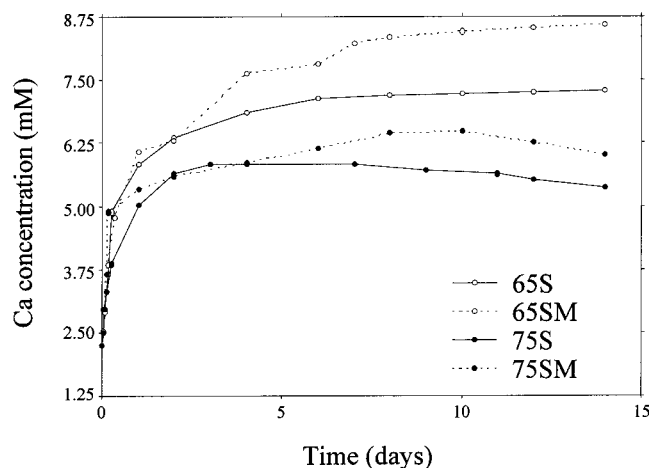


Figure 5. Calcium concentration in the SBF vs soaking time.

small at the beginning of the process. However, beyond 2 or 3 days the concentration of this element is slightly higher for the substrate containing magnesium. Therefore, the inhibitory effect of this element on the growth of the phosphate layer cannot be attributed to an eventual depletion of Ca²⁺ in the solution. In regard to this, it has to be considered that besides the chemical composition of the solution in contact with the substrate, the formation of the apatite layer on glass surfaces may also be governed by their textural properties, particularly pore size and surface area.^{3,4} For pure silica glasses, it has been reported that a reduction of the average pore size below 2 nm results in a strong decrease of the crystallization rate of the phosphate layer.¹¹ Although it remains to be determined whether this conclusion applies also for calcium-containing glasses, it could be safely assumed that in our case the phosphate growing would not be limited by the pore size, which is well above 2 nm in the four glasses. Indeed, it has been reported that the bioactivity depends on surface area, and it is not controlled by pore size for glasses with $d_p > 2.6$ nm.¹² As has been shown above, the surface area increases with the magnesium content of the glass, but nevertheless the presence of this element affects in a negative manner the growth of apatite. This behavior then suggests that not all the glass surface areas could be equally active in nucleating the apatite crystals. Following this hypothesis, it would be most useful to characterize the chemical nature of the glass surface. This has to be done by means of X-ray photoelectron spectroscopy (XPS).

X-ray Photoelectron Spectroscopy (XPS). The phosphorus 2p XPS spectra of the four glasses consist of one signal centered at 133.4 ± 0.2 eV, which corresponds to PO₄³⁻ groups.¹³ The P 2p in hydroxyapatite is detected at the same binding energy.¹³ The binding energy of Ca²⁺ 2p_{3/2}, 347.4 ± 0.2 eV, characteristic of this ion in common salts, was the same in all samples, as well as the band shape. The Si 2p band appears at a binding energy of 103.3 ± 0.2 eV, characteristic of this

element tetrahedrally coordinated by four oxygen atoms. The magnesium, whenever present, is detected at 51.0 ± 0.2 eV, characteristic of this element in an oxygen environment.

The oxygen 1s XPS spectra of the glasses are shown in Figure 6, where the spectra of an hydroxyapatite sample has been included as reference. These experimental spectra can be deconvoluted into two components, centered at 531.3 ± 0.2 eV and 533.1 ± 0.2 eV, respectively. The first peak appears at the same binding energy as the O 1s peak in hydroxyapatite,^{13,14} whereas the one at 533.1 eV corresponds to oxygen in a silica environment.¹⁵ Therefore, the XPS results indicate that the glass surface is highly heterogeneous, and clearly suggest the existence of calcium phosphate microdomains, where the calcium, oxygen, and phosphorus environments are quite similar to those present in hydroxyapatite. These results are not surprising, owing to the well-known general stability of calcium phosphates and, on the contrary, the reluctance of phosphorus to form P–O–Si bonds if divalent or trivalent ions are also present.

The XPS analysis also reveals strong differences in chemical composition between the bulk and the glass surface (see Table 1). In general, the surface is poorer in calcium than the bulk, but contains more phosphorus (except for sample 75S). Indeed, these differences are enhanced as the glasses become richer in silica. On the other hand, the addition of magnesium results in a strong increase of phosphorus at the surface, and at the same time a high level of magnesium is also detected. Since the presence of magnesium produces a modest increase of calcium (samples 75S and 75SM) or even a depletion of this element (sample 65SM compared with 65S), the preferential association of magnesium with phosphate at the glass surface would explain the ejection of phosphorus from the interior to the more external rim of the glass particles, whenever they contain magnesium. Indeed, it is worth mentioning that the sample with the highest concentration of magnesium at the surface (65SM) exhibits the lowest bioactivity.

Transmission Electron Microscopy (TEM). The identification by XPS of calcium, phosphorus, and oxygen in chemical environments analogous to those present in calcium phosphate-type materials, led us to investigate the microstructure of the glasses by means of TEM and EDS.

The TEM-EDS analysis at a 30-nm scale of grains shows strong differences in chemical composition among different regions of the glasses under examination. In the cases where phosphorus, calcium, and silicon are detected in the same area, their relative proportions change from one region to another. Also, regions with no phosphorus at all are found, but interestingly wherever this element is detected, calcium is present as well. Moreover, for the magnesium-free samples, crystals with a filamentous morphology can be clearly distinguished at the border of grains. These crystals turn out to be composed of calcium, phosphorus, and oxygen only (Figure 7, sample 65S). The electron dif-

(11) Pereira, M. M.; Clark, A. E.; Hench, L. L. *J. Am. Ceram. Soc.* **1995**, *78*, 2463.

(12) Li, R.; Clark, A. E.; Hench, L. L. *Chemical Processing of Advanced Materials*; Hench, L. L., West, J. K., Eds.; John Wiley & Sons: New York, 1992; p 627.

(13) Ong, J. L.; Lucas, L. C.; Raikar, G. N.; Weimer, J. J.; Gregory, J. C. *Colloids Surf. A. Phys. Eng. Aspects* **1994**, *87*, 151.

(14) Amrah-Bouali, S.; Rey, C.; Lebugle, A.; Bernache, D. *Biomaterials* **1994**, *15*, 151.

(15) Carriere, B.; Deville, J. P.; Brion, D.; Escard, J. *J. Electron Spectrosc.* **1977**, *10*, 85.

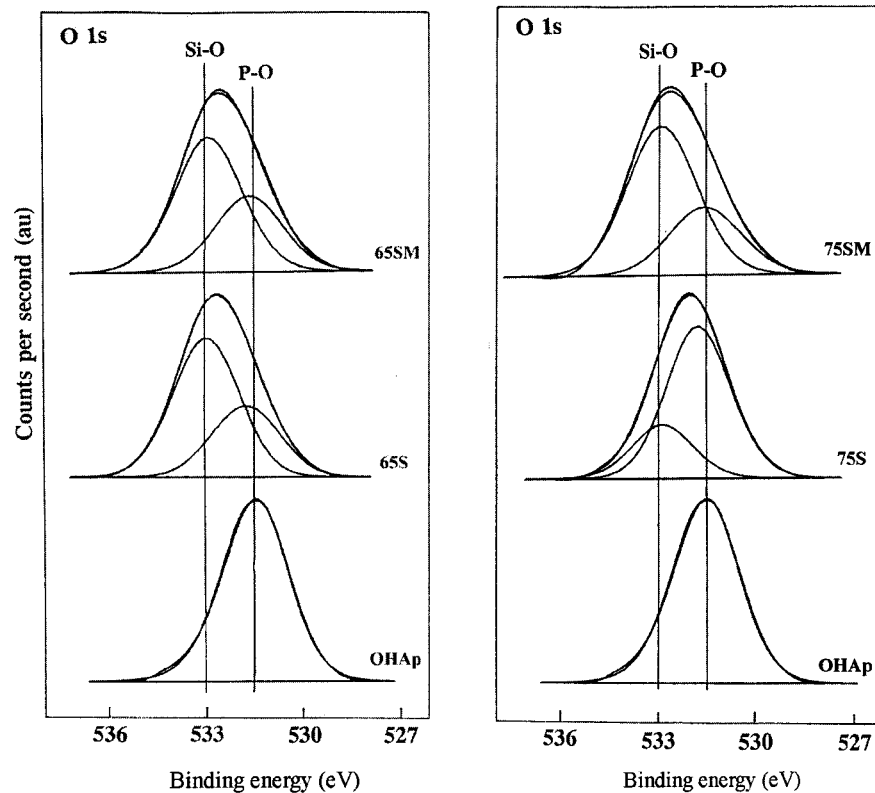


Figure 6. XPS spectra of oxygen 1s of the glasses and the reference sample of hydroxyapatite.

Table 1. Bulk and Surface (XPS) Atomic Compositions for the Calcined Disks of Glass

	atom %							
	bulk				surface (XPS)			
	Si	P	Ca	Mg	Si	P	Ca	Mg
65S	62.5	7.7	29.8	0	70.1	11.7	18.1	0
65SM	62.5	7.7	24.0	5.8	61.2	14.9	12.5	11.3
75S	72.1	7.7	20.2	0	88.8	3.9	7.3	0
75SM	72.1	7.7	16.3	3.8	76.9	10.2	9.3	3.5

fraction pattern of these crystals is also presented in Figure 7. This pattern, although rather diffuse, shows the basic diffraction features of hydroxyapatite and, hence, can be assigned to this phase.

In the two glasses containing magnesium, this element is detected always together with calcium, phosphorus, and silicon. Indeed, only one region consisting of calcium phosphate crystals has been found among the several examined. Therefore, the magnesium seems to inhibit the formation of these domains. Furthermore, according to the XPS results, the magnesium is preferentially associated with phosphate. Then, taking into account also the magnitude of the area analyzed by EDS (~30 nm), the magnesium would be probably present as calcium magnesium phosphate particles of nanometric size.

The preferential association of calcium and phosphorus to build up calcium phosphate, which appears as apatite-type microdomains in the silica matrix, as revealed by XPS and TEM-EDS, would not be surprising, owing to the well-known stability of the resulting calcium silicate and calcium phosphate phases. The formation of these phases would be the driving force to arrange the glass at nanometric scale. The presence of such microdomains in the glasses should have a strong

impact on their bioactivity, since they would act as preferred nucleation centers for apatite crystallization. Indeed, it has been discussed by Wang et al.⁸ that the key role that the interfacial energy between the nucleus and the substrate plays in the nucleation of apatite crystals on monocrystalline silicon. These authors show that an apatite film in a preferred orientation [102] can be grown on a Si(111) oriented surface, whereas a Si(100) surface remains inactive. The difference was attributed to the crystallographic matching between the Si(111) and the apatite crystals in [102] orientation. In our case, if apatite crystals were already present in the glass, they would offer the minimum interfacial energy for apatite growth, acting as nucleation centers for the crystallization of this phase. In addition, the inhibitory effect of the magnesium on the formation of the layer on the glass can be attributed to its negative influence on the formation of the apatite nucleation centers, as evidenced by TEM.

Finally, it has to be understood that the preferred crystallization of apatite onto the nuclei previously existing on the substrate does not completely exclude its eventual nucleation on other regions of the glass. Indeed, the high supersaturation of the environment with regard to apatite also provides a strong driving force for its nucleation, even if the interfacial energy with the substrate is not particularly low.

Conclusions

It has been found in glasses prepared by a sol-gel procedure in the system $\text{SiO}_2\text{-CaO}\cdot\text{P}_2\text{O}_5$ that the surface area increases, whereas the average pore size decreases from 7 to 3 nm as the silica content increases from 65 to 75 mol %. The addition of magnesium ($\text{Ca/Mg} = 4.1$) to the glasses causes an increase in surface area and

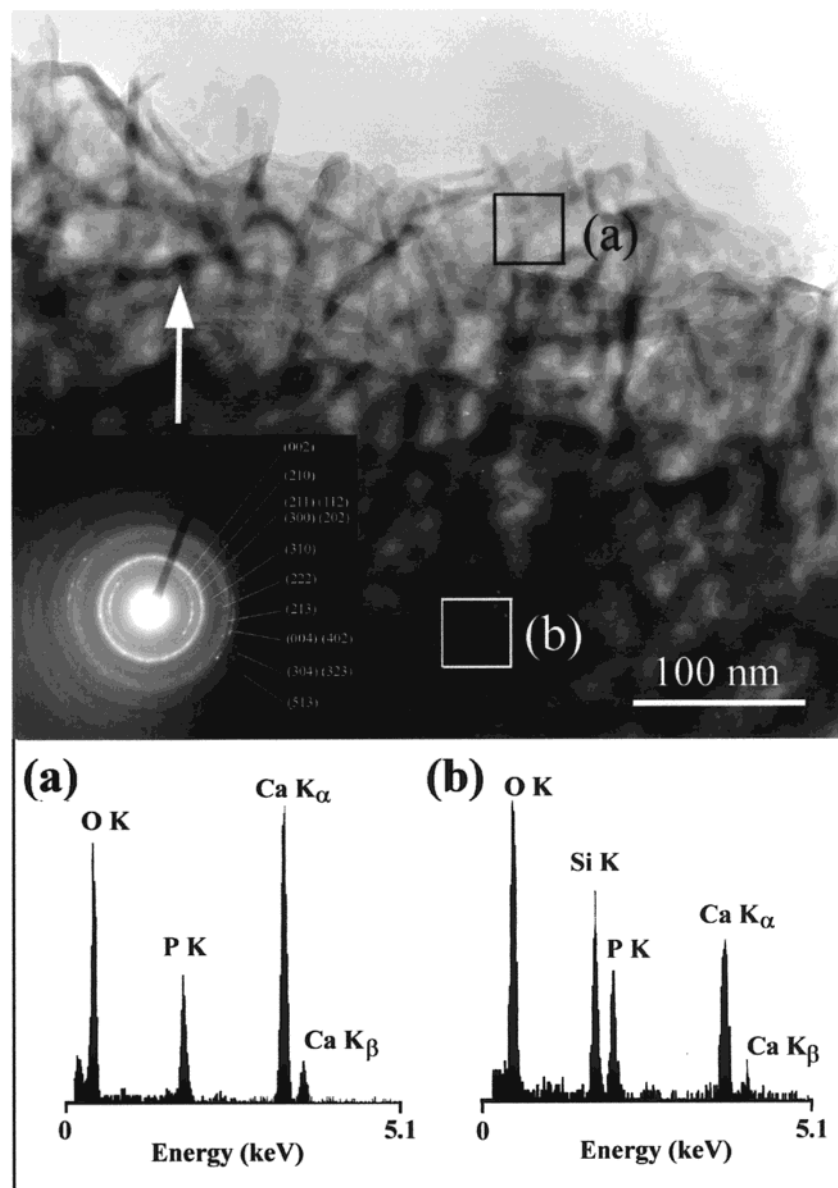


Figure 7. TEM image for glass 65S. TEM-EDS spectra for (a) external and (b) internal regions in the glass particle. The inset shows the ED pattern acquired for a selected area region a.

pore volume, whereas a very small reduction in pore sizes is observed.

The glasses develop an apatite layer by soaking in a SBF solution, but a retarding influence of the magnesium on the formation rate of this layer is found.

XPS shows the presence of calcium, phosphorus, and oxygen in an apatite-like environment at the surface of the glasses, reveals strong differences between bulk and surface chemical compositions, and suggests a preferential association of phosphorus with magnesium whenever this element is present at the glass surface.

TEM examination of the magnesium-free glasses shows the presence of pure calcium phosphate domains, whose electron diffraction pattern matches that of

apatite. These phosphate regions are barely detected in the glasses containing magnesium. These calcium phosphate microdomains are proposed to be preferential nucleation centers for the crystallization of apatite under the conditions prevalent in the *in vitro* tests.

Acknowledgment. The authors acknowledge to Dr. J. García Fierro for collecting and discussing the XPS spectra. The authors are grateful for financial support provided by Comisión Interministerial de Ciencia y Tecnología (CICYT) through MAT99-0466 research project. Thanks also to Dr. A. Gómez Herrero and Dr. F. Conde for technical advising.

CM9911114